

# Game theoretic modeling of helping behavior in emergency evacuations

Jaeyoung Kwak<sup>1,\*</sup>, Michael H. Lees<sup>2</sup>, Wentong Cai<sup>3</sup>, Ahmad Reza Pourghaderi<sup>4,6</sup>, and Marcus E.H. Ong<sup>5,6</sup>

<sup>1</sup> *Complexity Institute, Nanyang Technological University, Singapore*

<sup>2</sup> *Informatics Institute, University of Amsterdam, The Netherlands*

<sup>3</sup> *School of Computer Science and Engineering, Nanyang Technological University, Singapore*

<sup>4</sup> *Health Systems Research Center (HSRC), Singapore Health Services, Singapore*

<sup>5</sup> *Department of Emergency Medicine, Singapore General Hospital, Singapore and*

<sup>6</sup> *Health Services and Systems Research (HSSR), Duke-NUS Medical School, Singapore*

(Dated: December 23, 2024)

We study the collective helping behavior in a room evacuation scenario in which two volunteers are required to rescue an injured person. We propose a game theoretic model to study the evolution of cooperation in rescuing the injured persons. We consider the existence of committed volunteers who do not change their decision to help the injured persons. With the committed volunteers, all the injured persons can be rescued depending on the payoff parameters. In contrast, without the committed volunteers, rescuing all the injured persons is not achievable on most occasions because some lonely volunteers often fail to find peers even for low temptation payoff. We have quantified various collective helping behaviors and summarized those collective patterns with phase diagrams. In the context of emergency evacuations, our study highlights the vital importance of the committed volunteers to the collective helping behavior.

## I. INTRODUCTION

Emergency evacuation simulations have received much attention since Helbing *et al.* [1] characterized collective phenomena in escape panic based on numerical simulations of self-driven many-particles. Some studies have stated that when people are escaping from the place of danger, they tend to move faster than their normal speed and behave in an individualistic manner, which may lead to people pushing each other [1–4]. In the majority of studies, numerical simulations of emergency evacuation were developed based on such assumptions. In view of this, various pedestrian emergency evacuation studies were performed, for instance, predicting total evacuation time in a class room [5] and preparing an optimal evacuation plan for a large scale pedestrian facility [6].

However, other studies have presented evidence that evacuees helped injured persons to escape the place of danger, for instance, the WHO concert disaster occurred on December 3, 1979 in Cincinnati, Ohio, United States [7] and the 2005 London bombings in United Kingdom [8]. Researchers have investigated helping behavior in emergency evacuation by means of pedestrian simulations. For instance, von Sivers *et al.* [9, 10] applied social identity theory to pedestrian simulation in order to simulate helping behavior observed in the 2005 London bombings. In their studies, they assumed that all the evacuees share the same social identity which makes them willing to help others rather than be selfish.

Although several studies focused on simulating helping behavior in emergency evacuations, little attention has been paid to the strategic interactions among evacuees. When an evacuee is helping an injured person to escape, the evacuee's helping behavior can be seen as an attempt to increase a collective good. This is especially true when

there are not enough dedicated rescue personnel, in such circumstances other evacuees may help one another. At the same time, helping an injured person can be a costly behavior because the volunteering evacuee spends extra time and takes a risk to assist the injured person. If the evacuee feels that helping behavior is a costly behavior for him, he might not help the injured person.

Game theory is a useful tool to predict how individuals decide their strategy in response to others' strategy. Under game theoretic assumptions, individuals are likely to select a strategy in a way to maximize their own payoff. Various game theoretical models have been applied for emergency evacuation simulations, for example, prisoner's dilemma game [11], snowdrift game [12], spatial game [13, 14], and evolutionary game [15]. In our previous study [16], we employed the volunteer's dilemma game [17, 18] to study the impact of volunteering cost on collective helping behavior in emergency evacuations. We observed different patterns of collective helping behaviors by changing volunteering cost parameter. Nevertheless, little is known about how the existence of volunteers can lead to behavioral changes of bystanders. One can imagine that, through strategic interactions, the presence of committed volunteers may influence on other evacuees to also help injured people. In this way one might observe a spread of helping behavior. On the other hand, in situations where two volunteers are needed to help an injured person, an individual volunteer might give up helping the injured person if he cannot find a potential partner.

In this work, we propose an evolutionary game theoretic model to examine the dynamics of evacuees behavior influenced by other evacuees. We perform numerical simulations for a room evacuation scenario in which two volunteers are required to move an injured person to the place of safety. In our numerical simulations, each evacuee updates his strategy after strategic interactions with other evacuees within his sensory range while the evacuee moves in the room. Hence, the spatial formation of individuals and the strategic interactions between the

\* jaeyoung.kwak@ntu.edu.sg

TABLE I. Payoff of a volunteer (C) and a bystander (D) in a two-player game. Here,  $R$  is the reward for mutual cooperation,  $P$  is the punishment for mutual defection,  $T$  is the temptation to defect, and  $S$  is the sucker's payoff. The entities indicate the payoff for the row player.

	Volunteer	Bystander
Volunteer (C)	$R$	$S$
Bystander (D)	$T$	$P$

individuals are coupled together in our numerical study. We consider the existence of committed volunteers who do not change their decision to rescue the injured persons. We characterize the collective helping behavior by systematically controlling the game payoff parameters along with the altruism strength. By means of numerical simulations, we observe different collective patterns of helping behavior in a room emergency evacuation scenario depending on the existence of committed volunteers and the value of control parameters. We quantify different collective helping behaviors based on the simulation results. We then study the well-mixed population model to better interpret the numerical simulation results. The evolutionary game theoretic model and its numerical simulation setups are explained in Section II. We then present and explain the simulation results with phase diagrams in Section III. Finally, we discuss the findings of this study in Section IV.

## II. MODEL

Our agent-based model consists of a game theoretical model and a movement model. The game theoretical model evaluates the probability that a bystander would turn into a volunteer helping an injured person. The evolutionary game model enables us to reflect the behavioral changes of an individual based on the behavior of other evacuees. The movement model calculates the sequence of pedestrian positions for each simulation time step. In this section, we explain the details of our game theoretical model and the numerical simulation setup.

### II.1. Evolutionary game model

We employ an evolutionary game model to study the behavioral change of players influenced by other players. As in our previous study [16], we consider two strategies of ambulant pedestrians: volunteer (C) and bystander (D). A volunteer (C) helps an injured person to evacuate while a bystander (D) does not help the injured person. In line with the two-player game, the payoff of individual  $i$ 's strategy can be presented in a payoff matrix in Table I. When individual  $i$  meets individual  $j$ , there are four types of payoff depending on strategy of each individual. If both the individuals are volunteers (C), they receive a reward for mutual cooperation, denoted by  $R$ .

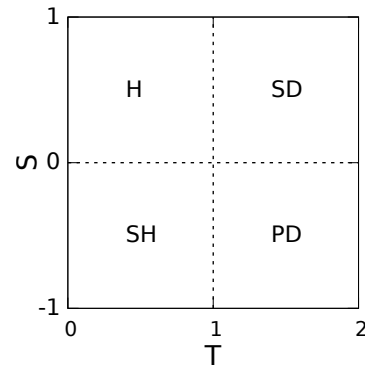


FIG. 1. Schematic representation of four different games on  $(T, S)$  space: the Harmony (H), the Snowdrift (SD), the Prisoner's dilemma (PD), and the Stag hunt (SH) games.

When both of them are bystanders (D), their payoff is  $P$  which is punishment for mutual defection. When bystander  $i$  is a volunteer (C) and bystander  $j$  is a bystander (D), bystander  $i$  receives the sucker's payoff  $S$  which is associated with the unreciprocated cooperation cost [19]. At the same time, bystander  $j$  receives  $T$  which reflects the temptation to defect. According to previous work [20–22], the  $(T, S)$  space can be divided into four areas: the Harmony (H), the Snowdrift (SD), the Prisoner's dilemma (PD), and the Stag hunt (SH) games [see Fig. 1].

We assume that two volunteers are required to move an injured person from the room to the place of safety. A lonely volunteer cannot move the injured person by himself, so he will try to find another volunteer who will move the injured person together. A bystander near the lonely volunteer might decide to become a volunteer to help the lonely volunteer to move the injured person together. In contrast, the lonely volunteer might give up finding another volunteer and turn into a bystander.

In the presented evolutionary game, player  $i$  considers not only his own payoff but also player  $j$ 's payoff. As suggested by [21, 23], we express the effective payoff of player  $i$ ,  $u_i$ , as a linear combination of player  $i$ 's and  $j$ 's payoffs:

$$u_i = (1 - Q)\pi_i + Q\pi_j, \quad (1)$$

where  $\pi_i$  and  $\pi_j$  denote the payoff of player  $i$  and  $j$  presented in Table I, respectively. The altruism strength  $Q$  reflects how much player  $i$  regards player  $j$ 's payoff, which is related to the degree of inequality aversion [24]. For simplicity, all the players are assumed to have the same  $Q$  value. Table II shows the effective payoff of a volunteer (C) and a bystander (D) according to Eq. 1.

In each round, ambulant pedestrian  $i$  randomly selects a neighbor  $j$  and adopts the neighbor  $j$ 's strategy with the probability [25–27]:

$$p(\Delta u_{ij}) = \frac{1}{1 + \exp(\Delta u_{ij}/k)}, \quad (2)$$

where  $k$  reflects uncertainties in the game dynamics and  $\Delta u_{ij} = u_i - u_j$  is payoff difference. In case of  $k = 0$ , the

TABLE II. The effective payoff of a volunteer (C) and a bystander (D) in the presented evolutionary game. Here,  $Q$  is the altruism strength reflecting how much player  $i$  regards player  $j$ 's payoff [21, 23, 24]. The entities indicate the payoff for the row player.

	Volunteer (C)	Bystander(D)
Volunteer (C)	$R_e = R$	$S_e = (1 - Q)S + QT$
Bystander (D)	$T_e = (1 - Q)T + QS$	$P_e = P$

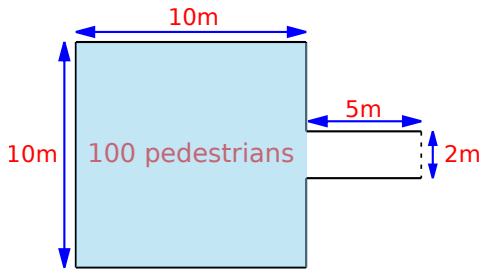


FIG. 2. Schematic depiction of the numerical simulation setup. 100 pedestrians are placed in a 10m×10m room indicated by a blue shade area. Pedestrians are leaving the room through an exit corridor which is 5 m long and 2 m wide. The place of safety is set on the right, outside of the exit corridor.

probability  $p(\Delta u_{ij})$  becomes 1 if  $u_i < u_j$ , and  $p(\Delta u_{ij})$  is 0 when  $u_i > u_j$ . In case of  $k \rightarrow \infty$ , the probability  $p(\Delta u_{ij})$  becomes 0.5, indicating completely random decision making.

## II.2. Social force model

We describe the movement of pedestrians based on the social force model [28]. The position and velocity of each pedestrian  $i$  at time  $t$ , denoted by  $\vec{x}_i(t)$  and  $\vec{v}_i(t)$ , are updated according to the following equations:

$$\frac{d\vec{x}_i(t)}{dt} = \vec{v}_i(t) \quad (3)$$

and

$$\frac{d\vec{v}_i(t)}{dt} = \vec{f}_{i,d} + \sum_{j \neq i} \vec{f}_{ij} + \sum_B \vec{f}_{iB}. \quad (4)$$

In Eq. (4), the driving force term  $\vec{f}_{i,d}$  describes the tendency of pedestrian  $i$  moving toward his destination. The repulsive force terms  $\vec{f}_{ij}$  and  $\vec{f}_{iB}$  reflect his tendency to keep certain distance from other pedestrian  $j$  and the boundary  $B$ , e.g., wall and obstacles. We refer the readers to Appendix A for further detailed description of the presented social force model.

## II.3. Numerical simulation setup

Each pedestrian is modeled by a circle with radius  $r_i = 0.2$  m. We placed  $N_0 = 100$  pedestrians in a

TABLE III. Game theoretic model parameters

Model parameter	symbol	value
mutual cooperation payoff	$R$	1
mutual defection payoff	$P$	0
temptation payoff	$T$	[0, 1]
sucker's payoff	$S$	[-1, 1]
altruism strength	$Q$	[0, 0.5]
sensory range	$l_s$	3
uncertainty parameter	$k$	0.25

10m×10m room indicated by a blue shaded area in Fig. 2. Pedestrians are leaving the room through an exit corridor which is 5 m long and 2 m wide. The place of safety is set on the right, outside of the exit corridor. The pedestrian movement is updated with the social force model in Eq. (4) [see Appendix A for more details].

There are  $N_i = 10$  injured persons who need a help in escaping the room and  $N = N_0 - N_i = 90$  ambulant pedestrians who are either volunteers or bystanders. In the beginning of numerical simulations, one volunteer is selected for each injured person from the set of his neighboring pedestrians within the sensory range  $l_s$ , thus there are  $N_{c,0} = 10$  initial volunteers. As described in Section II.1, we assume that an injured person needs two volunteers, thus the maximum number of volunteers is 20. We have performed numerical simulations for the cases without and with committed volunteers. In the case without committed volunteers, the initial volunteers can change their strategy in the simulations. In the other case, where the initial volunteers are committed, the initial volunteers do not change their strategy. The number of volunteers evolves according to the result of strategic interaction with other evacuees.

All the ambulant pedestrians play the presented evolutionary game at each 0.1 second. Each ambulant pedestrian  $i$  randomly selects pedestrian  $j$  within the sensory range  $l_s$  and then evaluates the probability of switching to pedestrian  $j$ 's strategy according to Eq. (2). Once a bystander interacts with a lonely volunteer and decides to cooperate with the lonely volunteer to rescue an injured person, the bystander turns into a volunteer. Next, the new volunteer shifts his desired walking direction vector toward the position of injured person. After arriving at the injured person, the new volunteer will evacuate the injured person with the peer volunteer after a preparation time of 5 s. On the other hand, if a lonely volunteer decides to become a bystander, then he changes his desired walking direction vector toward the exit. To implement the presented game theoretic model, the parameter values in Table III are selected based on the previous work [21, 26, 29]. Note that we control the game payoff parameters  $T$  and  $S$  along with the altruism strength  $Q$ .

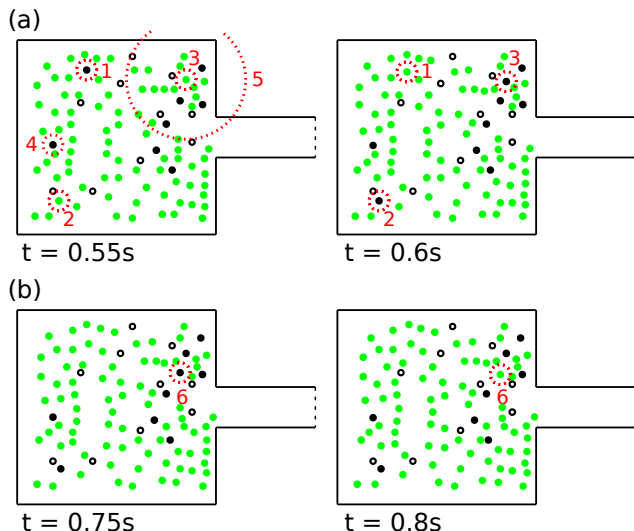


FIG. 3. Representative examples of individual strategy changes in the numerical simulations. The individuals changing their strategy are indicated by red dotted circle lines. Open black circles indicate the injured persons and full dark circles denote the volunteers helping the injured persons. Green circles represent the bystanders. The presented snapshots are captured from pedestrian trajectories generated from the case without committed volunteers with  $T = 0.1$ ,  $S = 0.1$ , and  $Q = 0$ . (a) A lonely volunteer (indicated by red dotted circle 1) at simulation time  $t = 0.55$  s (left) turns into a bystander at simulation time  $t = 0.6$  s (right). At the same time, two bystanders indicated by red dotted circles 2 and 3 at simulation time  $t = 0.55$  s (left) become volunteers at simulation time  $t = 0.6$  s (right), seemingly due to the influence of nearby volunteers in red dotted circles 4 and 5, respectively. (b) Similarly to (a), another lonely volunteer indicated by red dotted circle 6 at simulation time  $t = 0.75$  s (left) gives up rescuing an injured person and become a bystander at simulation time  $t = 0.8$  s (right).

### III. RESULTS AND DISCUSSIONS

The presented game theoretic model is studied by means of numerical experiments. We present the results from agent-based simulations. We then study a well-mixed population model to interpret the presented results.

#### III.1. Agent-based simulations

From the numerical experiments, we can see individuals who change their strategy as a result of interaction with their neighbors, refer to Fig. 3. As can be seen from Fig. 3(a), two bystanders become volunteers seemingly due to the influence of volunteers near them. At the same time, a lonely volunteer turns into a bystander after interacting with a nearby bystander. In Fig. 3(b), similarly to the observation presented in Fig. 3(a), one can see that a lonely volunteer gives up rescuing an injured person and becomes a bystander after interacting with a nearby bystander. In the case with committed volun-

teers, one can also see the change of individual strategy as shown in Fig. 3

To quantify the level of collective helping behavior, similarly to Ref. [11], we define a normalized fraction of cooperators  $n_c \in [-1, 1]$  as

$$n_c = \frac{N_c - N_{c,0}}{N_{c,0}}, \quad (5)$$

where  $N_c$  and  $N_{c,0}$  are the number of volunteers in the stationary state and in the initial condition, respectively. A positive value of  $n_c$  suggests that the number of volunteers  $N_c$  is greater than the initial one,  $N_{c,0}$ , inferring that some lonely volunteers successfully find peer volunteers. In case of  $n_c = 1$ , all the lonely volunteers eventually find their peers, thus all the injured persons are rescued. A negative value indicates that some lonely volunteers changed their mind to become bystanders. In case of  $n_c = -1$ , all the lonely volunteers turn into bystanders, so none of the injured persons are rescued. The stationary state values of  $n_c$  in the  $(T, S)$  space are presented in Appendix B.

Representative time series of the fraction of cooperators  $n_c$  in the case without committed volunteers are presented in Fig. 4. The curves in Fig. 4(a) and Fig. 4(b) are generated with the same parameter combination of  $T$ ,  $S$ , and  $Q$  but different sets of random seeds. As can be seen from Fig. 4(a), the stationary state value of  $n_c$  is positive but smaller than 1. In Fig. 4(b), the stationary state value of  $n_c$  reaches to 1, suggesting that all the lonely volunteers successfully find peer volunteers, thus all the injured are rescued. However, this complete rescue is not always possible in that the number of volunteers in the stationary state is changing depending on the random seeds. As shown in Fig. 4(c), the stationary state value of  $n_c$  is 0, inferring that the number of volunteers is not increased in effect. In Fig. 4(d),  $n_c$  becomes negative, implying that some lonely volunteers turn into bystanders, thus some injured persons are not rescued. Figure 4(e) presents that  $n_c$  decreases to  $-1$ , suggesting that none of the injured are rescued because all the lonely volunteers turn into bystanders.

Figure 5 shows same graphs as Fig. 4(a)-(c) but for the case with committed volunteers. As indicated by Fig. 5(a), the stationary state value of  $n_c$  becomes 1 when  $T$  is low and  $S$  is high for a given  $Q$ . That is, all the lonely volunteers successfully find peer volunteers, thus all the injured are rescued. For intermediate values of  $T$  and  $S$ , the  $n_c$  curve increases as in Fig. 5(a) but the stationary state value is smaller than 1. This indicates that some lonely volunteers successfully find peers while other lonely volunteers fail to do that, see Fig. 5(b). When  $T$  is high and  $S$  is low, as can be seen from Fig. 5(c), the value of  $n_c$  curve does not increase.

In the context of emergency evacuations, it is interesting to examine whether all the injured persons are rescued. We characterize different patterns of collective helping behavior by means of  $P_r$  which denotes the probability of complete rescue. We measure the value of  $P_r$  by counting the occurrence of complete rescue over 100

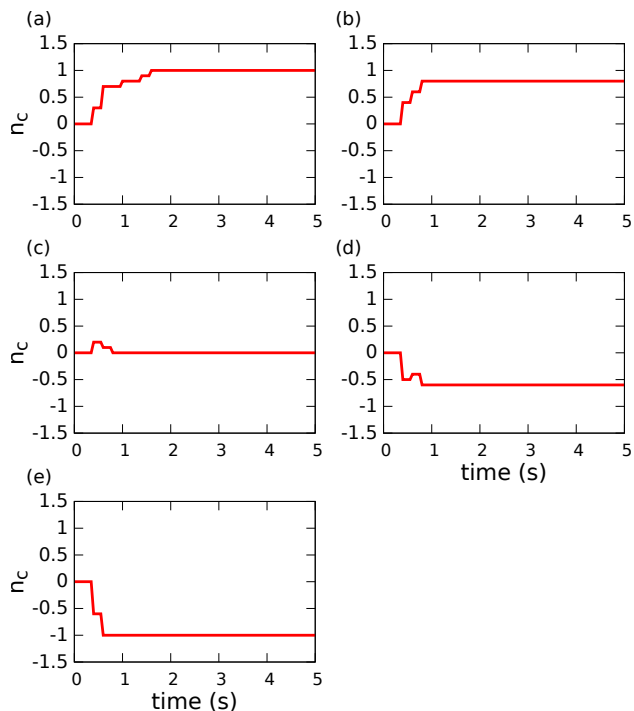


FIG. 4. Representative time series of the fraction of cooperators  $n_c$  in the case without committed volunteers. (a) The  $n_c$  curve (generated with  $T = 0.1$ ,  $S = 0.95$ , and  $Q = 0$ ) reaches to 1, indicating that all the lonely volunteers successfully find peer volunteers, thus all the injured are rescued. (b) The  $n_c$  curve generated from the same parameter combination of  $T$ ,  $S$ , and  $Q$  as (a), but with a different set of random seeds. The value of  $n_c$  increases in the course of time, but the stationary state value is smaller than 1. This implies that some lonely volunteers successfully find peers while other lonely volunteers fail to do so, thus not all the injured persons are rescued. (c) The stationary state value of  $n_c$  is 0, showing that the number of volunteers is not increased in effect. The presented curve is generated with  $T = 0.1$ ,  $S = 0.15$ , and  $Q = 0$ . (d) The  $n_c$  curve becomes negative, inferring that some lonely volunteers turn into bystanders, thus some injured persons are not rescued. Here, the curve is generated with  $T = 0.1$ ,  $S = -0.15$ , and  $Q = 0$ . (e) The  $n_c$  curve ( $T = 0.1$ ,  $S = -0.75$ , and  $Q = 0$ ) decreases to  $-1$ , suggesting that none of the injured are rescued because all the lonely volunteers turn into bystanders.

independent simulation runs for each parameter combination  $(T, S)$  along with a given value of  $Q$ . Based on the value of  $P_r$ , we define three phases: full cooperation, partial cooperation, and defection phases. The full cooperation phase is characterized by  $P_r = 1$ , suggesting that the complete rescue is always achievable regardless of random seeds. One can identify the partial cooperation phase with  $1 > P_r > 0$ , in which the complete rescue can be seen depending on random seeds. The defection phase is characterized by  $P_r = 0$ , implying that the complete rescue is not observable from simulation results. In the case without committed volunteers [see Fig. 6], the complete rescue probability  $P_r$  is always 0, indicating that the full cooperation phase does not exist. In addition, the value of  $P_r$  becomes smaller as  $Q$  grows for a given

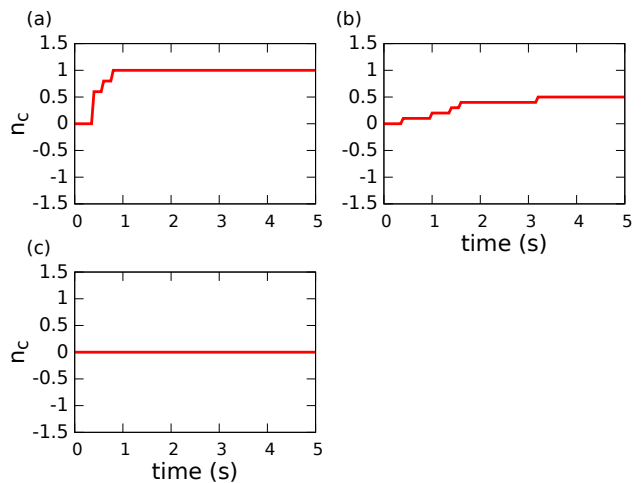


FIG. 5. Same graphs as Figs. 4(a)-(c) but for the case with committed volunteers. (a) When  $T$  is low and  $S$  is high for a given  $Q$ , the stationary state value of  $n_c$  is 1, suggesting that all the lonely volunteers successfully find peer volunteers, thus all the injured are rescued. The presented curve is generated with  $T = 0.3$ ,  $S = 0.5$ , and  $Q = 0$ . (b) For intermediate level of  $T$  and  $S$ , the  $n_c$  curve increases like in (a) but the stationary state value is smaller than 1, indicating that some lonely volunteers successfully find peers while other lonely volunteers fail to do that. The presented  $n_c$  curve is obtained with  $T = 0.8$ ,  $S = 0.1$ , and  $Q = 0$ . (c) If  $T$  is high and  $S$  is low, the value of  $n_c$  curve does not increase, denoting that the number of volunteers is not increased in effect. The presented curve is generated with  $T = 1.7$ ,  $S = -0.5$ , and  $Q = 0$ .

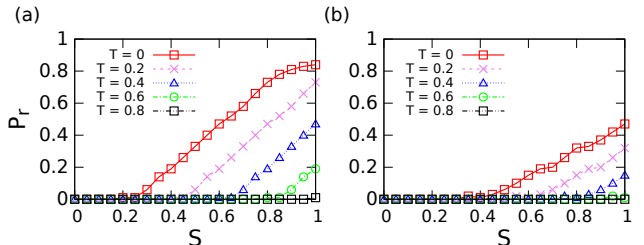


FIG. 6. Complete rescue probability  $P_r$  in the case without committed volunteers as a function of  $S$  and  $T$  for different values of  $Q$ : (a)  $Q = 0$  (low level) and (b)  $Q = 0.2$  (intermediate level). The case of high  $Q$  is not presented here because  $P_r$  is always zero for the entire  $(T, S)$  space, implying that a complete rescue is not possible. For each parameter combination of  $(T, S)$ , increasing  $Q$  yields lower  $P_r$ . In the case without committed volunteers,  $P_r = 1$  is not realized.

value of  $(T, S)$ . In the case with committed volunteers [refer to Fig. 7],  $P_r$  becomes 1 with high values of  $S$  when  $Q$  is at low level. This suggests the existence of full cooperation phase, see Fig. 7(a). For high level of  $Q$ , the value of  $P_r$  tends to approach 1, but  $P_r$  is still smaller than 1. This implies that the full cooperation phase is not observable when  $Q$  is high.

Figure 8 summarizes numerical results of phase characterizations. The parameter space of  $(T, S)$  is divided into different phases by means of the complete rescue probability  $P_r$ . In the case without committed volunteers [see

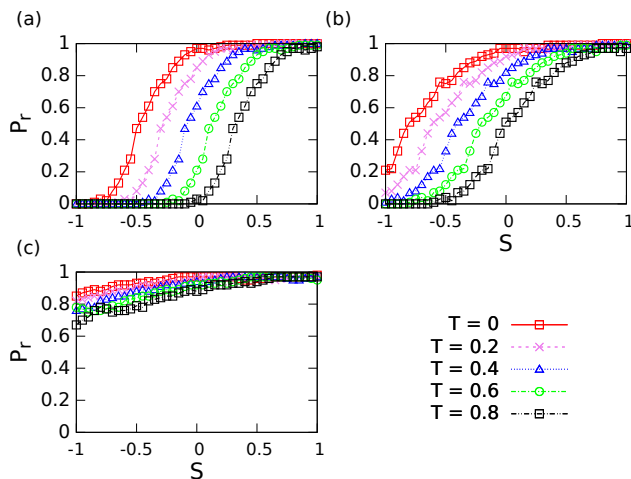


FIG. 7. Complete rescue probability  $P_r$  in the case with committed volunteers as a function of  $S$  and  $T$  for different values of  $Q$ : (a)  $Q = 0$  (low level), (b)  $Q = 0.2$  (intermediate level), and (c)  $Q = 0.4$  (high level). Similarly to the case without committed volunteers,  $P_r$  increases against  $S$  for a given  $T$ . One can see  $P_r = 1$  for high  $S$  with low  $T$  and  $Q$ , but it is not observable if  $Q$  is above a certain value.

Figure 8(a)], if  $Q$  is small, the partial cooperation phase can be observed in a limited area of  $(T, S)$  but the cooperation phase is not observed. The area of partial cooperation phase is getting smaller as  $Q$  increases and becomes invisible when  $Q = 0.4$ . At the same time, the defection phase is expanding in the  $(T, S)$  space as  $Q$  grows. From Figure 8(b), when  $Q$  is small, one can observe the full cooperation phase for high  $S$  and low  $T$ , corresponding to the Harmony (H) game. In addition, the defection phase is widely observed in the Prisoner's dilemma (PD) game and can be seen from some  $(T, S)$  combinations in the Snowdrift (SD) and the Stag hunt (SH) games. As  $Q$  grows, the area of partial cooperation phase is expanding while the defection phase area is decreasing. At the same time, surprisingly, increasing  $Q$  eventually leads to the disappearance of full cooperation phase. This can be understood that increasing  $Q$  contributes to the spreading of cooperation, but some lonely volunteers still fail to find a peer volunteer. This is apparently because the altruism strength  $Q$  reduces the payoff difference between the cooperator and defector. Consequently, the probability that a bystander switches to a volunteer is reduced. In terms of the two-player game, increasing  $Q$  makes all the games (i.e., H, SD, SH, and PD games) result in the partial cooperation phase, thus the collective helping behavior becomes insensitive to the values of  $S$  and  $T$ .

### III.2. Interpretation in terms of well-mixed population model

Some of the results presented in Section III.1 can be interpreted in terms of the well-mixed population model. Based on the well-mixed population model, we study the evolution of the number of cooperators  $N_C$  without con-

sidering the spatial formation of individuals. The evolution of  $N_C$  is given as

$$N_C(t + \Delta t) = N_C(t) + \frac{dN_C(t)}{dt} \Delta t, \quad (6)$$

where  $dN_C(t)/dt$  is the time derivative of the number of cooperators at time  $t$  and  $\Delta t$  is the time step. At  $t = 0$ ,  $N_C(t)$  is given as  $N_{C,0}$  denoting the initial number of cooperators. If  $dN_C(t)/dt$  is positive, the number of cooperators  $N_C(t)$  is going to increase. Negative  $dN_C(t)/dt$  leads to the decrement of  $N_C(t)$ , so  $N_C(t)$  in the stationary state is likely smaller than  $N_{C,0}$ . Note that, in our study,  $dN_C(t)/dt$  is a function of payoff parameters  $T$  and  $S$  along with the altruism strength  $Q$ . We refer the readers to Appendix C for further details relate to Eq. (6).

In the case without committed volunteers, the majority of numerical simulations result in the defection phase, see Fig. 8(a). According to Eq. (6), this is seemingly because of the negative value of  $dN_C(t)/dt$  in the beginning of numerical simulations. Consequently, the number of cooperators decreases in the course of time, leading to the loss of volunteers.

In the case with committed volunteers [see Fig. 8(b)], partial and full cooperation phases are frequently observed over a larger area of  $(T, S)$  space. This suggests that  $dN_C(t)/dt$  is mostly positive in the beginning of numerical simulations. In addition, due to the committed volunteers,  $dN_C(t)/dt$  does not become negative irregardless of payoff parameters  $T$  and  $S$ , implying that the stationary state value of  $N_C$  is equal or larger than  $N_{C,0}$ .

It is generally accepted that the well-mixed population model often fails to predict complex collective phenomena observed from numerical simulations due to its major limitation. The well-mixed population model is not able to consider the spatial formation of individuals, thus the heterogeneity in spatial structure cannot be reflected in the evolutionary game analysis. Previous studies [30, 31] have highlighted that the spatial structure is of great importance to the onset of collective cooperation behaviors. Unlike those previous studies, in this study, one can observe that the results from the presented well-mixed population approach is in good agreement with those from numerical simulations presented in Section III.1. This is seemingly because the evacuation scenario is studied for a small fixed square room and the mobility pattern of individuals is simple.

## IV. CONCLUSION

This paper presents a game theoretical model of helping behavior among evacuees. We have numerically investigated the evolution of collective helping behavior in a room evacuation scenario. In our numerical simulations, injured persons were placed in the room and it was assumed that each injured person needs the help of two volunteers during the evacuation. We assigned an initial volunteer to each injured person in the beginning

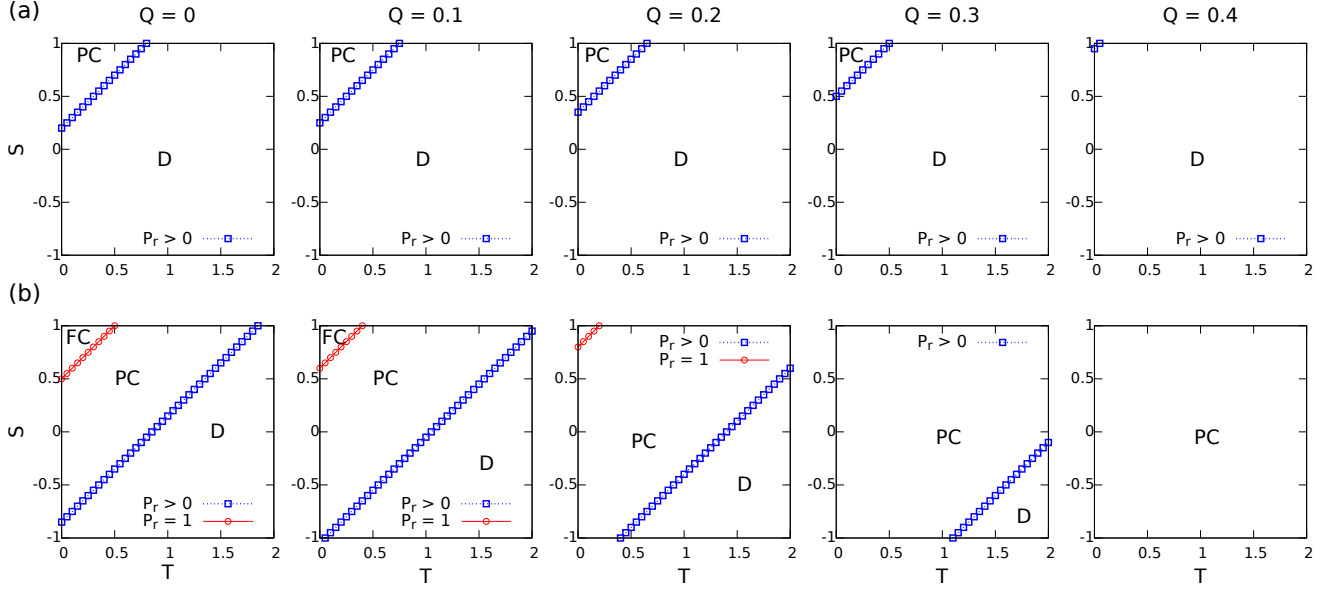


FIG. 8. Phase diagrams summarizing the numerical results: (a) the case without committed volunteers and (b) the case with committed volunteers. The  $(T, S)$  space is divided into different phases by means of the complete rescue probability  $P_r$ . Here, D, PC, and FC indicate the defection, partial cooperation, and full cooperation phases, respectively. Different symbols represent the boundaries between different phases: red circles ( $\circ$ ) for the boundary between FC and PC, and blue rectangles ( $\square$ ) for the boundary between PC and D. The full cooperation phase (i.e.,  $P_r = 1$ ) is not observed in the case without committed volunteers, but it can be seen in the case without committed volunteers for high  $S$  with low  $T$  and  $Q$ . In the case without committed volunteers, the area of partial cooperation (PC) phase shrinks as  $Q$  increases and is virtually disappeared when  $Q = 0.4$ . In the case with committed volunteers, in contrast, the area of partial cooperation phase is expanding as  $Q$  increases. In addition, the areas of full cooperation (FC) and defection (D) phases shrink and then disappear as  $Q$  increases.

of numerical simulations. The initial volunteers who do not changing their decision to rescue an injured person are indicated as committed volunteers. In this study, we considered the cases without and with committed volunteers. The initial volunteers can change their strategy in the case without committed volunteers, but it is not allowed in the case with committed volunteers. The number of volunteers evolved as a result of strategic interactions between individuals.

By systematically controlling payoff parameters and altruism strength, we characterized different collective helping behaviors. In the case without committed volunteers, we observed the partial cooperation phase for low temptation payoff  $T$  and high sucker's payoff  $S$  with low altruism strength  $Q$ . For high  $Q$ , the defection phase was widely observed in a wide area of  $(T, S)$  space, even in the Harmony game. However, different patterns were observed in the case with committed volunteers. For high  $S$  with low  $T$  and  $Q$ , the full cooperation phase was observed from the numerical simulations, in which all the injured persons were rescued regardless of random seeds. As  $Q$  increases, it was observed that the area of partial cooperation phase was expanding in the  $(T, S)$  space. Consequently, when  $Q$  was high, the whole  $(T, S)$  space became the partial cooperation phase, even in the Prisoner's dilemma game. It is suggested that the existence of committed volunteers can contribute to the appearance of full cooperation phase in low  $Q$  and expansion of partial cooperation phase in high  $Q$ . Increasing the al-

truism strength  $Q$  reduced the payoff difference between the cooperator and defector, leading to the spreading of defection phase in the case without committed volunteers and partial cooperation phase in the case of committed volunteers. Surprisingly, in the case with committed volunteers, increasing  $Q$  eventually also resulted in the disappearance of full cooperation phase. This is seemingly because increasing  $Q$  reduces the payoff difference between the cooperator and defector, thus the probability that a bystander switches to a volunteer is reduced.

The numerical simulation results of this study can be understood in line with the well-mixed population model. In the case with committed volunteers, the time derivative of the number of cooperators was mostly positive in the beginning of simulations. Consequently, we could often observe the partial and full cooperation phases. On the other hand, in the case without committed volunteers, the time derivative of the number of cooperators was negative on most occasions, leading to the loss of volunteers. In contrast to previous studies [30, 31], the analysis based on the well-mixed population model demonstrated a good agreement with our numerical simulation results. This is seemingly due to the simple mobility patterns of evacuees in a small fixed square room.

There are possible directions of future work addressing the limitations of this study. To focus on the essential features of the strategic interactions in helping behavior, this study has considered a simple room evacuation scenario. The presented model needs to be tested with more

complex geometry conditions to further examine complex nature of strategic interactions among individuals. In this study, the temptation payoff  $T$  and the sucker's payoff  $S$  were assumed to be same for the every evacuee. It would be interesting to introduce different values of  $T$  and  $S$  to each evacuee. For instance, the values of  $T$  and  $S$  can be given depending on the distance to the exit, speed reduction factor  $\alpha$ , or the estimated extra evacuation time incurred by helping the injured persons. In addition, it was assumed that each individual interacts with a random neighbor within the sensory range. According to Ref. [32], the emergence pattern of cooperation can be affected by the selection of interaction rule for the evolutionary game. This is apparently because changing to another interaction rule is likely to make a difference in evaluating the payoff difference with the interaction partners. One can consider other interaction rules, for instance, the stochastic interaction by which individuals can interact with several different players in each time step. Another possible direction of future work can be planned in line with the number of committed volunteers. In this study, we observed that the partial and full cooperation phases were widely spreading in the  $(T, S)$  space as a result of introducing committed volunteers. This study presented the difference between without and with committed volunteers, but did not investigate under which conditions the committed volunteers contribute to the appearance of system-wide cooperation. Previous studies [22, 33, 34] have examined under what conditions the committed minorities play a pivotal role in the emergence of cooperation in a well-mixed population and structured networks. In the context of pedestrian evacuations, the results and analysis from our approach can be extended to quantify the critical mass effect in collective helping behavior in terms of the number of committed volunteers.

### ACKNOWLEDGEMENTS

This research is supported by National Research Foundation (NRF) Singapore, GOVTECH under its Virtual Singapore Program Grant No. NRF2017VSG-AT3DCM001-031. We thank Mr. Vinayak Teoh Kannappan for his help in implementing the presented agent-based model with C++.

### Appendix A: Details of the social force model

In Section II.2, we presented a general form of the social force models [28, 35, 36]. This appendix provides further details of the presented social force model.

The social force models describe the acceleration of pedestrian  $i$  as a superposition of driving and repulsive force terms according to the following equation of motion:

$$\frac{d\vec{v}_i(t)}{dt} = \vec{f}_{i,d} + \sum_{j \neq i} \vec{f}_{ij} + \sum_B \vec{f}_{iB}. \quad (\text{A1})$$

TABLE IV. Social force model parameters

Model parameter	symbol	value
interpersonal repulsion strength	$C_p$	3.0
interpersonal repulsion range	$l_p$	0.2
normal elastic constants	$k_n$	50.0
tangential elastic constants	$k_t$	25.0
boundary repulsion strength	$C_b$	10.0
boundary repulsion range	$l_b$	0.1

The driving force  $\vec{f}_{i,d}$  is given as

$$\vec{f}_{i,d} = \frac{v_d \vec{e}_i - \vec{v}_i(t)}{\tau}, \quad (\text{A2})$$

where  $v_d$  is the desired speed and  $\vec{e}_i$  is a unit vector indicating the desired walking direction of pedestrian  $i$ . The relaxation time  $\tau$  controls how fast the pedestrian  $i$  adapts its velocity to the desired velocity.

The interpersonal repulsive force term  $\vec{f}_{ij}$  is specified according to the circular specification [35] which is the most simplistic form of the interpersonal repulsive interaction. The explicit form of  $f_{ij}$  can be written as

$$\vec{f}_{ij} = C_p \exp\left(\frac{r_i + r_j - d_{ij}}{l_p}\right) \vec{e}_{ij}, \quad (\text{A3})$$

where  $\vec{e}_{ij} = \vec{d}_{ij}/d_{ij}$  is a unit vector pointing from pedestrian  $j$  to pedestrian  $i$ , and  $\vec{d}_{ij} \equiv \vec{x}_i - \vec{x}_j$  is the distance vector pointing from pedestrian  $j$  to pedestrian  $i$ . The strength and the range of repulsive interaction between pedestrians are denoted by  $C_p$  and  $l_p$ , respectively. Instead of the circular specification, one might select a different form of specifications such as elliptical specification I (ES-1) [28] and elliptical specification II (ES-2) [36].

In addition to the interpersonal repulsive force term  $\vec{f}_{ij}$  presented in Eq. (A3), the interpersonal elastic force term  $\vec{g}_{ij}$  is added when the distance  $d_{ij}$  is smaller than the sum  $r_{ij} = r_i + r_j$  of their radii  $r_i$  and  $r_j$ . We describe  $\vec{g}_{ij}$  as Helbing [35] suggested,

$$\vec{g}_{ij} = h(r_{ij} - d_{ij}) \{k_n \vec{e}_{ij} + k_t [(\vec{v}_j - \vec{v}_i) \cdot \vec{t}_{ij}] \vec{t}_{ij}\}, \quad (\text{A4})$$

where  $k_n$  and  $k_t$  are the normal and tangential elastic constants, respectively. A unit vector  $\vec{e}_{ij}$  is pointing from pedestrian  $j$  to pedestrian  $i$ , and  $\vec{t}_{ij}$  is a unit vector perpendicular to  $\vec{e}_{ij}$ . The function  $h(x)$  yields  $x$  if  $x > 0$ , while it gives 0 if  $x \leq 0$ .

The repulsive force from boundaries  $\vec{f}_{iB}$  is given as

$$\vec{f}_{iB} = C_b \exp\left(-\frac{d_{iB}}{l_b}\right) \vec{e}_{iB}, \quad (\text{A5})$$

where  $d_{iB}$  is the perpendicular distance between pedestrian  $i$  and wall, and  $\vec{e}_{iB}$  is the unit vector pointing from the wall  $B$  to the pedestrian  $i$ . The strength and range of repulsive interaction from boundaries are denoted by  $C_b$  and  $l_b$ .

To implement the presented social force model, the parameter values in Table IV are selected based on the previous studies [28, 35, 37, 38].

The ambulant pedestrians move with the initial desired speed  $v_d = v_{d,0} = 1.2$  m/s and with relaxation time  $\tau = 0.5$  s, and their speed cannot exceed  $v_{\max} = 2.0$  m/s. Until now, the speed of volunteers rescuing the injured persons is often assumed by the modelers, like the work of von Sivers *et al.* [9, 10]. We applied speed reduction factor  $\alpha = 0.5$  to the volunteers rescuing the injured persons, so they move with a reduced desired speed  $v_d = \alpha v_{d,0} = 0.6$  m/s. Following previous studies [37, 39, 40], we discretized the numerical integration of Eq. (A1) using the first-order Euler method:

$$\vec{v}_i(t + \Delta t) = \vec{v}_i(t) + \vec{a}_i(t)\Delta t, \quad (\text{A6})$$

$$\vec{x}_i(t + \Delta t) = \vec{x}_i(t) + \vec{v}_i(t + \Delta t)\Delta t. \quad (\text{A7})$$

Here,  $\vec{a}_i(t)$  is the acceleration of pedestrian  $i$  at time  $t$  which can be obtained from Eq. (A1). The velocity and position of pedestrian  $i$  is denoted by  $\vec{v}_i(t)$  and  $\vec{x}_i(t)$ , respectively. The time step  $\Delta t$  is set as 0.05 s.

### Appendix B: Exploration of the $(T, S)$ space

In Section III.1, we presented the representative time series of the fraction of cooperators  $n_c$ : the case without committed volunteers [Fig. 4] and the case with committed volunteers [Fig. 5]. To complement the results presented in Figs. 4 and 5, we evaluate the stationary state values of  $n_c$  in terms of the average and standard deviation of  $n_c$ , i.e.,  $\mu(n_c)$  and  $\sigma(n_c)$ . The values of  $\mu(n_c)$  and  $\sigma(n_c)$  are measured over 100 independent simulation runs for a parameter combination of  $(T, S)$  with a fixed value of  $Q$ .

In the case without committed volunteers,  $\mu(n_c)$  grows as  $S$  increases for a given value of  $Q$ , indicating that high  $S$  leads to the increment of volunteers. The  $\sigma(n_c)$  curves increase and then decrease if  $Q$  is at low and intermediate levels, but the change of  $\sigma(n_c)$  against  $S$  is not significant when  $Q$  is high. In Fig. 9(a),  $\mu(n_c)$  is almost 1 when  $S$  is high and  $T$  is low, but  $\sigma(n_c)$  is not zero. This suggests that the complete rescue of all the injured persons is not always achievable, which is consistent with our observation from Fig. 4(a) and Fig. 4(b). In addition, if we increase  $Q$ , we can observe that the minimum value of  $\mu(n_c)$  is increasing while its maximum value is decreasing for given value of  $T$ . This is seemingly due to the increment of  $\sigma(n_c)$ . In Fig. 10, we present the average and standard deviation of the normalized fraction of cooperators in the  $(T, S)$  space. In line with the results in Fig. 9, the difference between minimum and maximum values of  $\mu(n_c)$  is decreasing while the value of  $\sigma(n_c)$  is growing as we increase  $Q$ .

In the case with committed volunteers, the  $\mu(n_c)$  curves show an increasing trend as  $S$  increases for a given value of  $Q$ , similarly to the case without committed volunteers. However, one can notice different patterns of  $\mu(n_c)$  and  $\sigma(n_c)$  curves when  $Q$  is high, see Fig. 11(c). It can be seen that  $\mu(n_c)$  is virtually 1 but smaller than 1. In addition,  $\sigma(n_c)$  is decreasing for increasing  $Q$ , but  $\sigma(n_c)$  does not become 0. This implies that the stationary state values of  $n_c$  is smaller than 1 even for high  $S$ ,

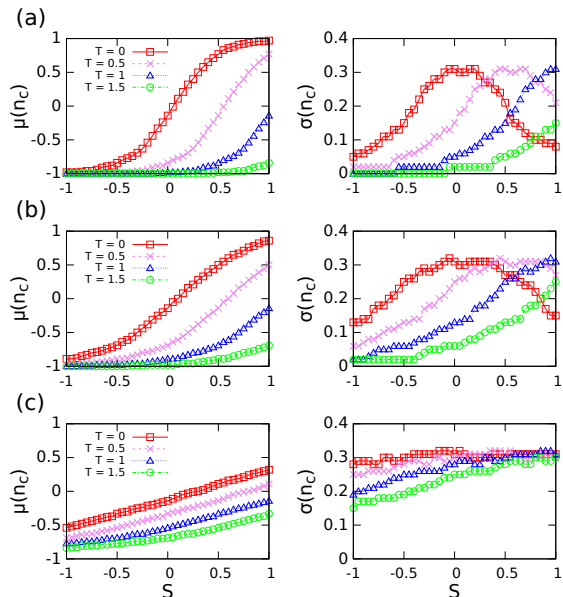


FIG. 9. Stationary state values of  $n_c$  in the case without committed volunteers: (a)  $Q = 0$  (low level), (b)  $Q = 0.2$  (intermediate level), and (c)  $Q = 0.4$  (high level). The average and standard deviation of the normalized fraction of cooperators, i.e.,  $\mu(n_c)$  and  $\sigma(n_c)$ , are presented in the left and right columns, respectively. Different symbols represent the different values of  $T$ . Results are evaluated over 100 independent simulation runs. For each given  $Q$ ,  $\mu(n_c)$  grows as  $S$  increases. The  $\sigma(n_c)$  curves increase and then decrease if  $Q$  is at low and intermediate levels, but the change of  $\sigma(n_c)$  against  $S$  is not significant when  $Q$  is high.

thus the complete rescue is not always possible. This is compatible with the results presented in Fig. 8(b). Figure 12 presents the numerical results of  $\mu(n_c)$  and  $\sigma(n_c)$  in the  $(T, S)$  space.

### Appendix C: Details of the well-mixed population model description

In Section III.2, we interpreted the numerical simulation results from the cases without and with committed volunteers. This appendix provides more details of our interpretation, especially how the well-mixed population model can explain the numerical simulation results.

Based on previous studies [22, 33, 34], we consider a well-mixed population model with a finite population consisting of  $N$  individuals. For the case without committed volunteers, the evolution of the number of cooperators,  $dN_C(t)/dt$ , can be described in terms of the increase rate  $f_+$  and decrease rate  $f_-$ ,

$$\frac{dN_C(t)}{dt} = f_+ - f_-. \quad (\text{C1})$$

The increase rate  $f_+$  is equal to the product of the pair selection probability  $p_s$  and the strategy adaption prob-

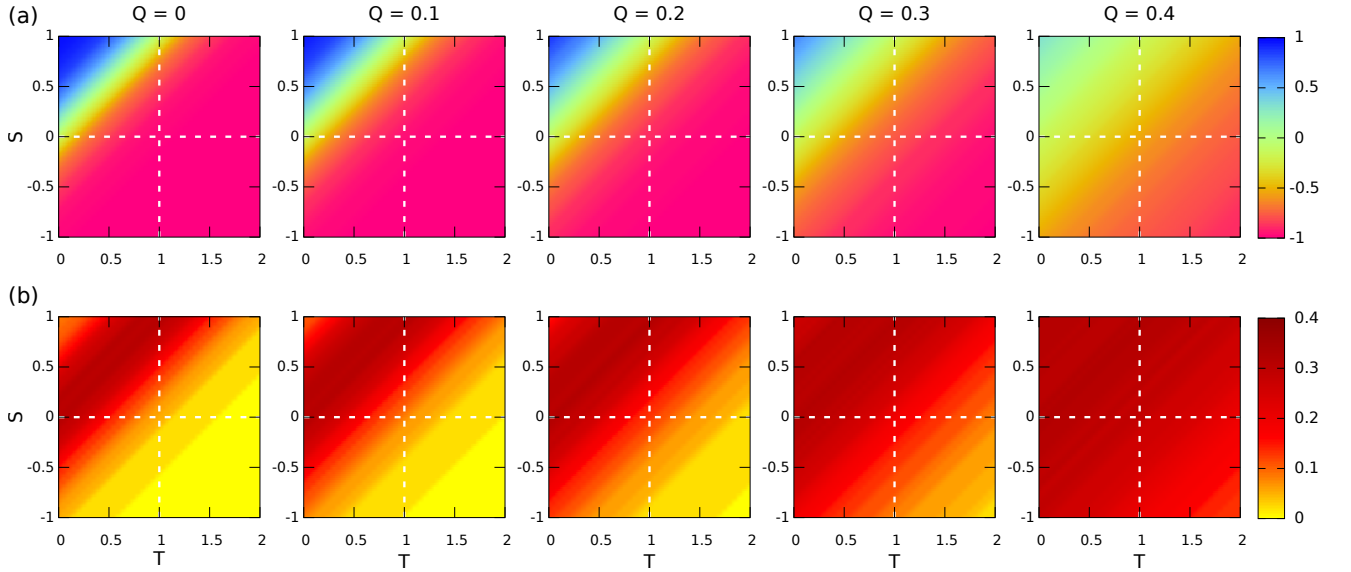


FIG. 10. The stationary state values of  $n_c$  for the case without committed volunteers in the  $(T, S)$  space: (a) average  $\mu(n_c)$  and (b) standard deviation  $\sigma(n_c)$ . Each panel corresponds to different values of altruism strength  $Q$ . Results are averaged over 100 independent simulation runs.

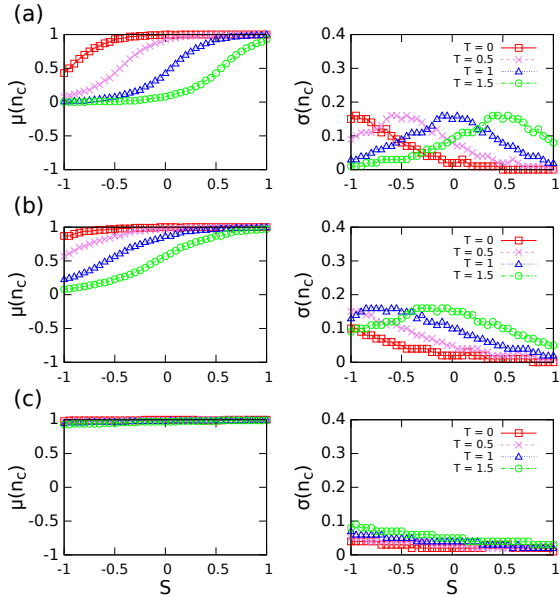


FIG. 11. Same graph as Fig. 9 but for the case with committed volunteers: (a)  $Q = 0$  (low level), (b)  $Q = 0.2$  (intermediate level), and (c)  $Q = 0.4$  (high level). Similarly to the case without committed volunteers, for a given value of  $Q$ , the  $\mu(n_c)$  curves show an increasing trend as  $S$  increases. However,  $\mu(n_c)$  is virtually 1 while  $\sigma(n_c)$  is small when  $Q$  is high, which is different from the case without committed volunteers.

ability  $p(\Delta u_{DC})$ :

$$f_+ = p_s p(\Delta u_{DC}) = \frac{N_C N_D}{N(N-1)} \frac{1}{1 + \exp[(T_e - S_e)/k]}, \quad (\text{C2})$$

where  $N$  is the number of ambulant pedestrians and  $N_C$  and  $N_D = N - N_C$  are the number of cooperators (i.e.,

volunteers) and defectors (i.e., bystanders), respectively. With the pair selection probability, we select a pair of players with different strategies, i.e., one player is a cooperator ( $C$ ) and the other one is a defector ( $D$ ). Here,  $\Delta u_{DC} = u_D - u_C$  is payoff difference obtained by subtracting from  $u_D$  to  $u_C$ . Note that the payoffs  $u_C$  and  $u_D$  are given as  $S_e$  and  $T_e$ , which are given in Table 1, respectively. Based on the strategy adaption probability, player  $i$  ( $D$ ) updates his strategy to player  $j$ 's one ( $C$ ), i.e., switching from  $D$  to  $C$ .

Likewise, the decrease rate  $f_-$  is given as

$$f_- = p_s p(\Delta u_{CD}) = \frac{N_C N_D}{N(N-1)} \frac{1}{1 + \exp[(S_e - T_e)/k]}. \quad (\text{C3})$$

Next, we check the trend of the number of cooperators  $N_C(t)$  in the course of time by looking into the sign of its change rate  $dN_C(t)/dt$ . As described in Section III.2, a positive value of  $dN_C(t)/dt$  possibly leads to the full or partial cooperation phases, while a negative value results in the defection phase. Based on Eqs. (C2) and (C3), we rewrite Eq. (C1) as

$$\frac{dN_C(t)}{dt} = \frac{N_C N_D}{N(N-1)} \left\{ \frac{1}{1 + \exp[(T_e - S_e)/k]} - \frac{1}{1 + \exp[(S_e - T_e)/k]} \right\}. \quad (\text{C4})$$

One can notice that the first term on the right-hand side is always positive for  $N > 1$  and  $N_C > 0$ , thus the sign of  $dN_C(t)/dt$  exclusively depends on the sign of  $p(\Delta u_{DC}) - p(\Delta u_{CD})$ . Fig. 13(a) presents the value of  $dN_C(t)/dt$  in the  $(T, S)$  space for different values of  $Q$ , comparable to the results presented in Fig. 10(a). As  $Q$  increases, the value of  $dN_C(t)/dt$  tends to decrease for a given value of  $T$  and  $S$ , suggesting the disappearance

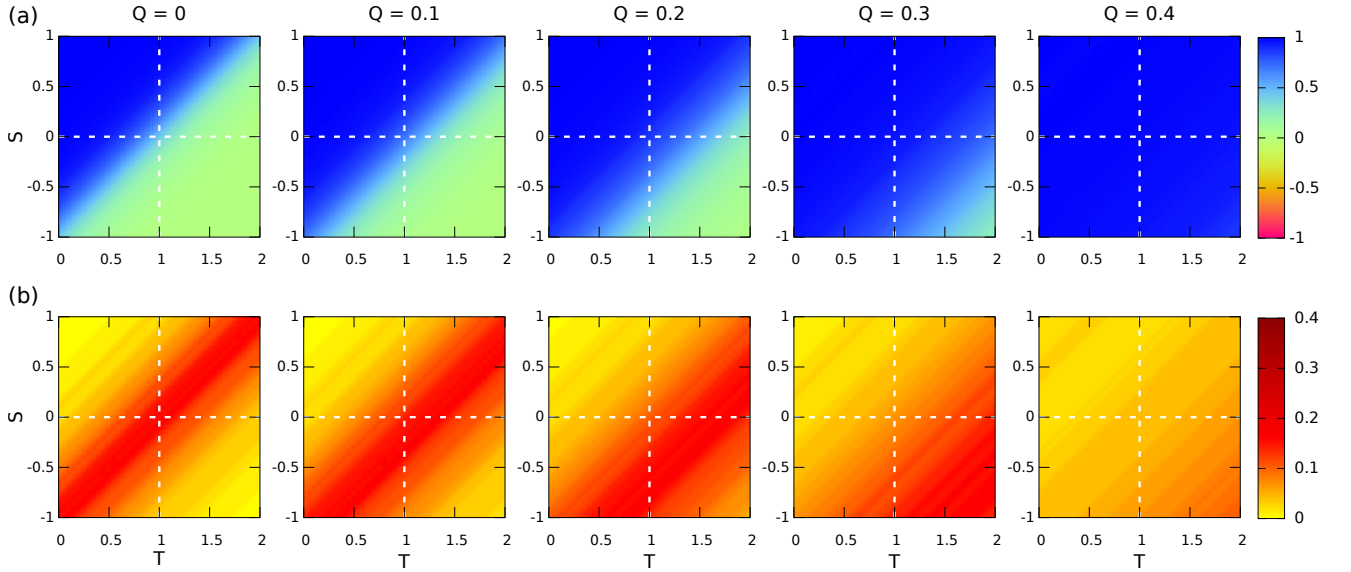


FIG. 12. The stationary state values of  $n_c$  for the case with committed volunteers in the  $(T, S)$  space: (a) average  $\mu(n_c)$  and (b) standard deviation  $\sigma(n_c)$ . Each panel corresponds to different values of altruism strength  $Q$ . Results are averaged over 100 independent simulation runs.

of partial cooperation phase and spreading of defection phase.

Now we focus on the case with committed volunteers. Like the case without committed volunteers,  $dN_C(t)/dt$  is described in terms of the increase rate  $f_+$  and decrease rate  $f_-$ , i.e.,  $dN_C(t)/dt = f_+ - f_-$  [Eq. (C1)]. Note that the committed volunteers do not update their strategy but they can induce defectors to become cooperators. The increase rate  $f_+$  is same as Eq. (C2), while the decrease rate  $f_-$  has to be modified. The sampling rate  $p_s$  is given as

$$p_s = \frac{(N_C - N_{C,0})N_D}{N(N-1)}, \quad (\text{C5})$$

where  $N_{C,0}$  is the initial number of volunteers. In the case with committed volunteers, all the initial volunteers are committed volunteers. Accordingly,  $(N_C - N_{C,0})$  denotes the number of volunteers who are not initial volunteers, indicating the number of volunteers who can change their strategy depending on the outcome of strategic interactions. The decrease rate  $f_-$  is modified as

$$f_- = \frac{(N_C - N_{C,0})N_D}{N(N-1)} \frac{1}{1 + \exp[(S_e - T_e)/k]}. \quad (\text{C6})$$

In the beginning of our numerical simulations,  $N_C$  is same as  $N_{C,0}$ , implying the decrease rate  $f_-$  becomes zero. The time derivative of  $N_C$  should read

$$\begin{aligned} \frac{dN_C(t)}{dt} &= \frac{N_C N_D}{N(N-1)} \frac{1}{1 + \exp[(T_e - S_e)/k]} \\ &\quad - \frac{(N_C - N_{C,0})N_D}{N(N-1)} \frac{1}{1 + \exp[(S_e - T_e)/k]}. \end{aligned} \quad (\text{C7})$$

Note that, for  $N_{C,0} > 0$ , Eq. (C7) is always larger than Eq. (C4), meaning that  $dN_C(t)/dt$  of the case with com-

mitted volunteers is higher than that of the case without committed volunteers. Furthermore, the value of  $dN_C(t)/dt$  is positive in the beginning of our numerical simulations, likely leading to the increment of  $N_C$ . Figure 13(b) shows  $dN_C(t)/dt$  in  $(T, S)$  space for different values of  $Q$ , showing qualitatively the same results as those presented in Fig. 12(a). As  $Q$  increases, the value of  $dN_C(t)/dt$  tends to decrease for high  $S$  and low  $T$  but increase for the rest of  $(T, S)$  space. This implies that the area of partial cooperation phase is expanding.

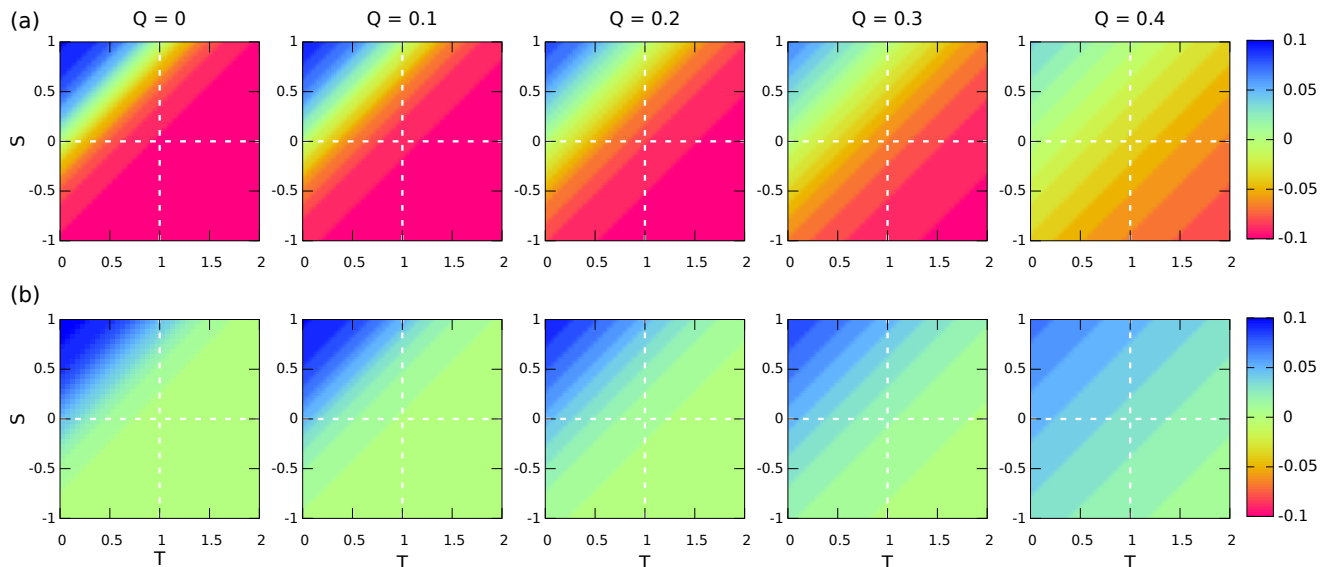


FIG. 13.  $dN_C(t)/dt$  in the  $(T, S)$  space computed in line with the well-mixed population model [see Eq. (C4)]: (a) the case without committed volunteers and (b) the case with committed volunteers. The presented results are generated with  $N = 90$  ambulant pedestrians,  $N_D = 80$  bystanders, and  $N_C = 10$  volunteers for (a) and  $N_{C0} = 10$  committed volunteers for (b). Each panel corresponds to different values of altruism strength  $Q$ .

- 
- [1] D. Helbing, I. Farkas, and T. Vicsek, Simulating dynamical features of escape panic, *Nature* **407**, 487 (2000).
- [2] A. Mintz, Non-adaptive group behavior, *The Journal of Abnormal and Social Psychology* **46**, 150 (1951).
- [3] H. Kelley, J. Condry Jr, A. Dahlke, and A. Hill, Collective behavior in a simulated panic situation, *Journal of Experimental Social Psychology* **1**, 20 (1965).
- [4] H. Braga and G. Moita, On the Boate Kiss fire and the Brazilian safety legislation: what we can learn, *Collective Dynamics* **2**, 1 (2017).
- [5] R. Guo, H. Huang, and S. Wong, Route choice in pedestrian evacuation under conditions of good and zero visibility: Experimental and simulation results, *Transportation Research Part B: Methodological* **46**, 669 (2012).
- [6] A. Abdelghany, K. Abdelghany, H. Mahmassani, and W. Alhalabi, Modeling framework for optimal evacuation of large-scale crowded pedestrian facilities, *European Journal of Operational Research* **237**, 1105 (2014).
- [7] N. Johnson, Panic at “The Who concert stampede”: an empirical assessment, *Social Problems* **3**, 362 (1987).
- [8] J. Drury, C. Cocking, and S. Reicher, The nature of collective resilience: survivor reactions to the 2005 London bombings, *International Journal of Mass Emergencies and Disaster* **27**, 66 (2009).
- [9] I. von Sivers, A. Templeton, G. Köster, J. Drury, and A. Philippides, Humans do not always act selfishly: Social identity and helping in emergency evacuation simulation, in *The Conference on Pedestrian and Evacuation Dynamics 2014 (PED 2014)*, edited by W. Daamen, D. Duives, and S. Hoogendoorn (Delft, The Netherlands, 2014) pp. 585–593.
- [10] I. von Sivers, A. Templeton, F. Künzner, G. Köster, J. Drury, A. Philippides, T. Neckel, and H. Bungartz, Modelling social identification and helping in evacuation simulation, *Safety Science* **89**, 288 (2016).
- [11] S. Bouzat and M. Kuperman, Game theory in models of pedestrian room evacuation, *Physical Review E* **89**, 032806 (2014).
- [12] D. Shi and B. Wang, Evacuation of pedestrians from a single room by using snowdrift game theories, *Physical Review E* **87**, 022802 (2013).
- [13] S. Heliövaara, H. Ehtamo, D. Helbing, and T. Korhonen, Patient and impatient pedestrians in a spatial game for egress congestion, *Physical Review E* **87**, 012802 (2013).
- [14] M. Mitsopoulou, N. Dourvas, G. Sirakoulis, and K. Nishinari, Spatial games and memory effects on crowd evacuation behavior with cellular automata, *Journal of Computational Science* **32**, 87 (2019).
- [15] Q. Hao, R. Jiang, M. Hu, B. Jia, and Q. Wu, Pedestrian flow dynamics in a lattice gas model coupled with an evolutionary game, *Physical Review E* **84**, 036107 (2011).
- [16] J. Kwak, M. Lees, W. Cai, and M. Ong, Modeling helping behavior in emergency evacuations using volunteer’s dilemma game, in *Lecture Notes in Computer Science*, Vol. 12137, edited by V. Krzhizhanovskaya, G. Závodszy, M. Lees, J. Dongarra, P. Sloot, S. Brissos, and J. Teixeira (Amsterdam, The Netherlands, 2020) pp. 513–523.
- [17] A. Diekmann, Volunteer’s dilemma, *Journal of Conflict Resolution* **29**, 605 (1985).
- [18] A. Diekmann and W. Przepiorka, “Take one for the team!” Individual heterogeneity and the emergence of latent norms in a volunteer’s dilemma, *Social Forces* **94**, 1309 (2016).
- [19] P. Smaldino, J. Schank, and R. McElreath, Increased cost of cooperation help cooperators in the long run, *The American Naturalist* **181**, 451 (2013).
- [20] D. Helbing and A. Johansson, Cooperation, norms, and revolutions: a unified game-theoretical approach, *PLOS ONE* **5**, e12530 (2010).

- [21] G. Szabo and A. Szolnoki, Selfishness, fraternity, and other-regarding preference in spatial evolutionary games, *Journal of Theoretical Biology* **299**, 81 (2012).
- [22] A. Cardillo and N. Masuda, Critical mass effect in evolutionary games triggered by zealots, *Physical Review Research* **2**, 023305 (2020).
- [23] T. Grund, C. Waloszek, and D. Helbing, How natural selection can create both self-and other-regarding preferences and networked minds, *Scientific Reports* **3**, 1 (2013).
- [24] E. Tricomi, A. Rangel, C. Camerer, and J. O'Doherty, Neural evidence for inequality-averse social preferences, *Nature* **463**, 1089 (2010).
- [25] G. Szabó and C. Tóke, Evolutionary prisoner's dilemma game on a square lattice, *Physical Review E* **58**, 69 (1998).
- [26] M. Amaral and M. Javarone, Heterogeneous update mechanisms in evolutionary games: mixing innovative and imitative dynamics, *Physical Review E* **97**, 042305 (2018).
- [27] W. Wang, Y. Lai, C. Grebogi, and J. Ye, Network reconstruction based on evolutionary-game data via compressive sensing, *Physical Review X* **1**, 021021 (2011).
- [28] D. Helbing and P. Molnár, Social force model for pedestrian dynamics, *Physical Review E* **51**, 4282 (1995).
- [29] Z. Wang and M. Perc, Aspiring to the fittest and promotion of cooperation in the prisoner's dilemma game, *Physical Review E* **82**, 021115 (2010).
- [30] Z. Wu and H. Yang, Social dilemma alleviated by sharing the gains with immediate neighbors, *Physical Review E* **89**, 012109 (2014).
- [31] H. Yang, Z. Wu, Z. Rong, and Y. Lai, Peer pressure: Enhancement of cooperation through mutual punishment, *Physical Review E* **91**, 022121 (2015).
- [32] B. Woelfing and A. Traulsen, Stochastic sampling of interaction partners versus deterministic payoff assignment, *Journal of Theoretical Biology* **257**, 689 (2009).
- [33] N. Masuda, Evolution of cooperation driven by zealots, *Scientific Reports* **2**, 646 (2012).
- [34] Y. Nakajima and N. Masuda, Evolutionary dynamics in finite populations with zealots, *Journal of Mathematical Biology* **70**, 465 (2015).
- [35] D. Helbing, Traffic and related self-driven many-particle systems, *Reviews of Modern Physics* **73**, 1067 (2001).
- [36] A. Johansson, D. Helbing, and P. Shukla, Specification of the social force pedestrian model by evolutionary adjustment to video tracking data, *Advances in Complex Systems* **10**, 271 (2007).
- [37] J. Kwak, H.-H. Jo, T. Luttinen, and I. Kosonen, Jamming transitions induced by an attraction in pedestrian flow, *Physical Review E* **96**, 022319 (2017).
- [38] J. Kwak, H.-H. Jo, T. Luttinen, and I. Kosonen, Collective dynamics of pedestrians interacting with attractions, *Physical Review E* **88**, 062810 (2013).
- [39] F. Zanlungo, T. Ikeda, and T. Kanda, Social force model with explicit collision prediction, *EPL (Europhysics Letters)* **93**, 68005 (2011).
- [40] F. Zanlungo, T. Ikeda, and T. Kanda, Potential for the dynamics of pedestrians in a socially interacting group, *Physical Review E* **89**, 012811 (2014).